

A Self-contained Approach to MEMS MARG Orientation Estimation for Hand Gesture Tracking in Magnetically Distorted Environments

Pontakorn Sonchan^(⊠), Neeranut Ratchatanantakit, Nonnarit O-larnnithipong, Malek Adjouadi, and Armando Barreto

Department of Electrical and Computer Engineering, Florida International University, Miami, FL, USA

{psonc001,nratc001,nolarnni,adjouadi,barretoa}@fiu.edu

Abstract. There is increasing interest in using low-cost and lightweight Micro Electro-Mechanical System (MEMS) modules containing tri-axial accelerometers, gyroscopes and magnetometers for tracking the motion of segments of the human body. We are specifically interested in using these devices, called "Magnetic, Angular-Rate and Gravity" ("MARG") modules, to develop an instrumented glove, assigning one of these MARG modules to monitor the (absolute) 3-D orientation of each of the proximal and middle phalanges of the fingers of a computer user. This would provide real-time monitoring of the hand gestures of the user, enabling non-vision gesture recognition approaches that do not degrade with lineof-sight disruptions or longer distance from the cameras. However, orientation estimation from low-cost MEMS MARG modules has shown to degrade in areas where the geomagnetic field is distorted by the presence of ferromagnetic objects (which are common in contemporary environments). This paper describes the continued evolution of our algorithm to obtain robust MARG orientation estimates, even in magnetically distorted environments. In particular, the paper describes a new self-contained version of the algorithm, i.e., one requiring no information from external devices, in contrast to the previous versions.

Keywords: MARG module · Orientation Estimation · Magnetic Disturbance

1 Motivation

1.1 Interest in Intuitive Means of Computer Input

The rising pervasiveness of virtual and augmented reality applications in human-computer interaction is currently driving an increasing interest in computer input mechanisms that are more natural and better matched to those environments [12]. There is an active search for methods to track the position and configuration of the user hands and fingers as a way to interact with the computer. Many of the approaches being investigated

are based on multi-camera vision systems. However, the introduction of Micro Electro-Mechanical System (MEMS) modules containing tri-axial accelerometers, gyroscopes, and magnetometers, in the past 20 years, seemed to, potentially, open up a completely different approach to hand tracking, with distinctive advantages and challenges.

1.2 Inertial and Magnetic Tracking Approach

The emergence of miniature MEMS accelerometers and gyroscopes in the 1990's and 2000's [3] sparked interest in their use for tracking segments of the human body in ways similar to the application of accelerometers and gyroscopes for navigational purposes, which had already been in practice for decades. This approach would be highly convenient for our goal of tracking of the articulated segments of a computer user's hand through a glove instrumented with several of these sensor modules [1, 8, 9, 13]. Unfortunately, it was discovered that the performance characteristics of the MEMS accelerometers and gyroscopes was much inferior with respect to their navigational counterparts. Soon MEMS magnetometers were added to the ensemble with the intent to improve the orientation estimation performance achievable by the sensor modules. Nonetheless, practice has shown that the same type of algorithms used for navigational tracking cannot be simply mapped to the MEMS MARG modules. New approaches have emerged that seek to use all the information available from the three sensor modalities contained by the MARG module.

We have previously developed the "Gravity Magnetic Vector with Double SLERP" (GMV-D) orientation estimation algorithm for MEMS MARG modules [10, 11, 16–18], where we emphasize the need to selectively increase or decrease the weight given to each of the sources of information in the module, according to the instantaneous operational conditions of the MARG.

In this paper we will first describe the GMV-D orientation estimation algorithm, overall. Then we will describe in detail how the trustworthiness parameters, α and μ , are obtained, with special emphasis on the novel approach taken to obtain values of μ that do not require any information from outside the MARG module for their computation. In the next sections we represent vectors and quaternions through boldface variables. In addition, we invoke a few well-established properties of quaternions as representations of 3-D rotations, which are fully developed in texts focused on the topic of quaternions, such as [2, 4] and [23].

2 The GMV-D MARG Orientation Estimation Algorithm

2.1 Conditional Involvement of Available Information Sources

Many of the previously proposed approaches for MARG orientation estimation seek to use all available forms of information (readings from all three types of sensors), to obtain a final orientation estimate. It seems, however, that the effective emphasis of most of the previous approaches is to "maximize" the involvement of the information sources in the estimation, targeting some theoretical goal in the estimate. For example, the Kalman Filter seeks to provide the linear estimator yielding the smallest variance in the estimate

[22]. However, many of the approaches do not deliberately include provisions to restrain or block the involvement of some forms of available information when those elements of information may not be trustworthy. The lack of such provisions could result in large estimate errors that persist for long intervals, given the fact that the estimate resulting from one iteration is fed back and used as a central factor in the estimation for the next iteration.

This may happen, for example, when the assumptions made for the use of signals such as accelerations and magnetic fields are not actually fulfilled at the moment in which they are used for the estimation. The alternative approach followed in our proposed method (GMV-D) is to assess, in every iteration of the algorithm, if the preconditions are met, and actively suppress the involvement of the corresponding sources of information, when they are not met. That is, GMV-D implements a form of conditional involvement of the available information sources.

2.2 Information Flow in the GMV-D Algorithm

The information flow through one iteration of the GMV-D algorithm is displayed in Fig. 1. At the beginning of each iteration, the latest set of gyroscope readings, \mathbf{w} , accelerometer readings \mathbf{a}_0 and magnetometer readings, \mathbf{m}_0 , will be read. The gyroscope readings, \mathbf{w} , will be first processed by a "De-biasing" stage, in which a linear model of the buffered samples of the gyroscope readings acquired during the most recent quasi-static interval is used to compensate for the possible bias in the gyroscope signals. This yields an "un-biased" set of angular rotation speeds, \mathbf{w}_B , which will be the ones effectively used for the algorithm. It should be noted that, historically, this kind of bias removal has been shown to be insufficient to eliminate the bias in gyroscope readings completely, and it is because we acknowledge the imperfection of this bias removal that the orientation estimation based on gyroscopic readings has to be corrected using other sources of information, in the GMV-D algorithm.

An initial (quaternion) orientation estimate, q_G , is defined by recursive integration of gyroscope measurements. To do this, the un-biased gyroscope readings are converted to a "quaternion rate of change", \dot{q} , as indicated in Eq. 1, where \otimes represents quaternion product and q_0 is the quaternion representing the orientation before the latest unbiased rotational speeds (cast as a quaternion) w_B , are considered. Then, the rate of change is "accumulated" (integrated) into the newest instantaneous gyroscope-based orientation quaternion, q_G , through Eq. 2, where Δt is the sampling interval and q_0^* is the quaternion conjugate of q_0 .

$$\dot{\mathbf{q}} = \frac{1}{2} \mathbf{q}_0 \otimes \mathbf{\omega_B} \tag{1}$$

$$\mathbf{q}_G = e^{\left((\Delta t)\dot{\mathbf{q}}\otimes\mathbf{q}_0^*\right)\otimes\mathbf{q}_0} \tag{2}$$

If the bias had been *completely* removed from w_B , this initial estimation of the orientation of the MARG would already be correct. However, unavoidable offset remnants in the gyroscope signals cause orientation "drift" in this q_G estimate that must be corrected periodically.

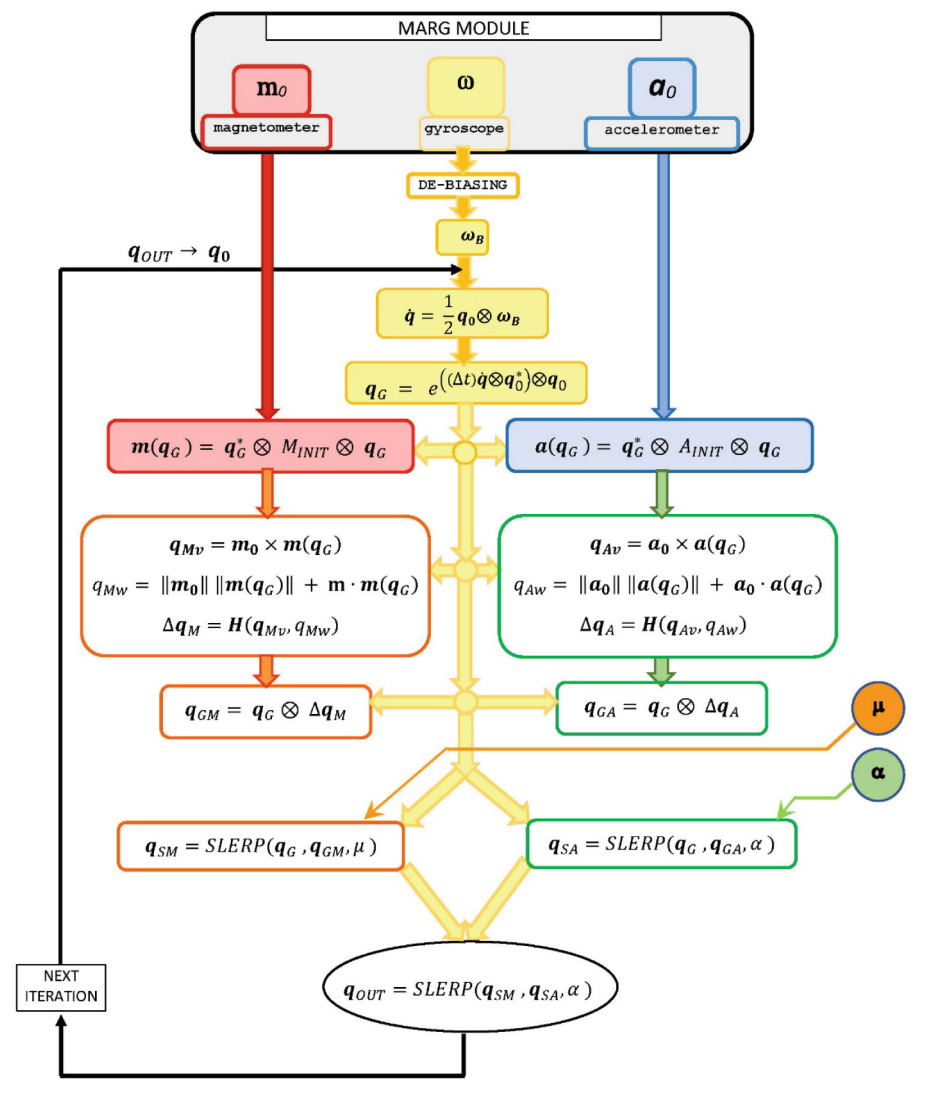


Fig. 1. Information flow during 1 iteration of the GMV-D MARG orientation estimation process. The computations of α and μ are explained in Sect. 3.

The two lateral columns shown in Fig. 1 symbolize the two pipelines of additional information that GMV-D implements to develop and apply quaternion correction components on the basis of magnetometer readings (left column) and accelerometer readings (right column). Both these pipelines have the same type of functionality. Therefore, only the right (accelerometer-based) pipeline will be described in detail at this point, letting the reader apply an analogous explanation to the functionality of the left (magnetometer-based) pipeline.

In GMV-D, both accelerometer-based and magnetometer-based corrections:

- 1. Are developed on the assumption of the existence of a uniform vector field,
- 2. Encode the degree to which the assumption is verified in a scalar parameter,
- 3. Use the parameter to modulate the significance of the corresponding correction.

The scalar trustworthiness parameters are α , for the accelerometer-based correction, and μ for the magnetometer-based correction, and each takes on values only in the closed interval [0, 1]. Their meaning and calculation will be detailed in subsequent sections. Here the basic explanation of GMV-D will assume that they are available in each iteration.

Observing the right pipeline in Fig. 1, we see that its objective is the computation of a quaternion orientation estimate, q_{GA} , which has been "fully" corrected on the basis of accelerometer readings. That is, q_{GA} is obtained by modifying the initial estimate, $q_{\rm G}$, by full application of an "acceleration orientation adjustment", $\Delta q_{\rm A}$, which will tweak the incrementally constructed quaternion to match the orientation informed by the current accelerometer readings. As detailed in [18], the quaternion, Δq_A , which encodes that additional rotation, can be inferred considering the (vector) cross product of the instantaneous acceleration measured, a_0 , and the direction of the acceleration vector that would be derived by mapping the initial measurement of the gravitational acceleration, A_{INIT} , to the current orientation of the body frame of the MARG, $a(q_G)$, which we call the "computed acceleration". A_{INIT} is the 3-dimensional vector recorded from the accelerometer readings at startup, when the orientation of the MARG body frame is adopted as the orientation of the fixed inertial frame, with respect to which the orientation of the body frame will be expressed, from that moment on. The mapping of A_{INIT} to the current orientation of the MARG body frame is calculated according to this useful property of quaternions [2, 4, 23], with q_G as the quaternion that represents the orientation of the second (body) frame, with respect to the first (inertial) frame.

$$a(q_G) = q_G^* \otimes A_{INIT} \otimes q_G \tag{3}$$

In the absence of gyroscope drift, the "computed acceleration", $a(q_G)$, would ideally match the measured instantaneous acceleration (gravity) in direction, so that no "orientation adjustment" (i.e., difference), Δq_A , would need to be considered. However, in the likely event that persistent residual gyroscope drift might have distorted the basic estimate of the MARG body frame, the vector and scalar parts of the additional orientation change, Δq_A , that could supplement the mapping of $A_{\rm INIT}$ to actually match a_0 can be computed as shown in Eqs. 4 (vector part) and 5 (scalar part).

$$\mathbf{q}_{A\mathbf{v}} = \mathbf{a}_0 \times \mathbf{a}(\mathbf{q}_G) \tag{4}$$

$$q_{Aw} = ||\boldsymbol{a}_0|| \ ||\boldsymbol{a}(\boldsymbol{q}_G)|| + \boldsymbol{a}_0 \cdot \boldsymbol{a}(\boldsymbol{q}_G)$$
 (5)

Then, Δq_A is obtained by concatenating both parts into a quaternion, as indicated by the H operator, in Eq. 6:

$$\Delta \mathbf{q}_A = \mathbf{H}(\mathbf{q}_{Av}, q_{Aw}) \tag{6}$$

Once this supplementary rotation quaternion, Δq_A , is obtained, it is effectively applied to define the quaternion q_{GA} , which encodes the MARG orientation estimate that assumes complete appropriateness of the accelerometer correction and has applied it to the latest available basic orientation estimate q_G :

$$\mathbf{q}_{GA} = \mathbf{q}_G \otimes \Delta \mathbf{q}_A \tag{7}$$

It should be noted that a completely analogous reasoning supports the computational steps illustrated on the left column of Fig. 1, to yield $q_{\rm GM}$, a quaternion encoding the results of modifying the original estimate of MARG orientation, $q_{\rm G}$, on the basis of applying a magnetometer-based correction in full. Similar to the process described for the right column of Fig. 1, except that referring to the magnetic field, a "computed magnetic vector" is obtained by now mapping the initial magnetic field recorded at startup, $\mathbf{M}_{\rm INIT}$, to the MARG body frame, using $q_{\rm G}$. The potential orientation "difference", $\Delta q_{\rm M}$, between the "computed magnetic vector" and the instantaneous output from the magnetometer is calculated with equations similar to Eqs. 4, 5 and 6, and then applied with an equation similar to Eq. 7. This yields $q_{\rm GM}$, a quaternion that represents the MARG orientation initially obtained from integration of gyroscopic signals but then fully corrected on the basis of instantaneous magnetometer readings,

At this point in the GMV-D iteration there are 3 prospective estimates for the MARG orientation: q_G , which was obtained merely updating the final MARG orientation estimate obtained from the previous iteration, q_0 , with the gyroscopic measurements from this iteration (in Eqs. 1 and 2); q_{GA} , the estimation in which the basic q_G , has been infused with information from the current accelerometer measurements, applying the accelerometer-based correction "fully"; and q_{GM} , the orientation estimate which has been infused with information from the current magnetometer measurements, applying the magnetometer-based correction "fully". It has already been pointed out that, in spite of the "de-biasing" procedure performed on the readings from the gyroscope, even w_B is likely to still contain persistent remnants of bias errors which will develop drift in q_G , unless it is corrected. Therefore, the corrections derived from accelerometer or magnetometer readings should be used, but only to the extent that the preconditions required in each of those corrections are met. Otherwise, an inadequate accelerometer-based or magnetometer-based correction would actually degrade the correctness of the orientation estimation further (for the current and future estimation results).

Figure 1 shows that GMV-D formulates the final orientation estimate as a combination of q_G , corrected using information from the accelerometer and q_G , corrected using information from the magnetometer, but only after the "strength" of each of these corrections is scaled in proportion to a single scalar trustworthiness parameter which is instantaneously assessed for each of the sources of information: $0 \le \alpha \le 1$ for the accelerometer correction and $0 \le \mu \le 1$ for the magnetometer correction. The specific meaning and formulation of these 2 parameters will be detailed in the next section, where the new approach for calculating μ without relying on signals that are external to the MARG module will be highlighted.

The scaling of the full-strength corrected orientation estimates, q_{GA} , and q_{GM} is implemented as quaternion interpolation from q_{G} to q_{GA} , controlled by α , and from q_{G} to q_{GM} , controlled by μ , respectively. In both cases the interpolation approach used is the

Spherical Linear Interpolation (SLERP), which is defined as follows for interpolating from a quaternion q_1 towards a quaternion q_2 , under control of the parameter h [21]:

$$\Omega = \cos^{-1}(\boldsymbol{q}_1 \cdot \boldsymbol{q}_2) \tag{8}$$

$$SLERP(q_1, q_2, h) = \frac{q_1 \sin((1 - h)\Omega) + q_2 \sin(h\Omega)}{\sin(\Omega)}$$
(9)

Therefore, the scaled accelerometer-corrected quaternion, q_{SA} , and the scaled magnetometer-corrected quaternion, q_{SM} , are given by:

$$\mathbf{q}_{SA} = SLERP(\mathbf{q}_G, \mathbf{q}_{GA}, \alpha) \tag{10}$$

$$\mathbf{q}_{SM} = SLERP(\mathbf{q}_G, \mathbf{q}_{GM}, \mu) \tag{11}$$

Figure 1 shows that GMV-D derives its final orientation estimate quaternion through a second tier of SLERP interpolation, from q_{SM} to q_{SA} , under control of α .

$$\mathbf{q}_{OUT} = SLERP(\mathbf{q}_{SM}, \mathbf{q}_{SA}, \alpha) \tag{12}$$

3 Formulation of the Trustworthiness Parameters

3.1 Accelerometer Correction Trustworthiness, \alpha

It is known that two "vector observations" are not sufficient to independently define the 3-D orientation of a moving rigid body [7]. However, our approach uses a pair of observations of the gravitational acceleration vector field (assumed constant throughout the operating space of the MARG) to infuse additional information into the MARG body orientation estimation, implementing a *correction* of q_G .

Within the context of our proposed application of MARG modules for hand tracking as an input mechanism for human-computer interaction, the local gravitational field is, indeed, uniform. That is, the vector representing the acceleration of gravity all around the prospective working space of the MARG can be considered as oriented perpendicular to the horizontal plane, pointing downwards, with the same magnitude. Unfortunately, the tri-axial accelerometer in the MARG does not exclusively respond to the gravitational acceleration, but, instead, the output of each of its 3 axes (X, Y and Z), will contain projections of the so-called "linear acceleration" superimposed on the components of the gravitational accelerations they sense. This "linear acceleration" refers to the acceleration that the MARG experiences when it is in movement, with a varying speed. Therefore, accelerometer-based corrections imply the presumption of immobility in association with both "vector observations" used for them, which are, in reference to Fig. 1, (an average) of the acceleration measured at startup, $A_{\rm INIT}$, and the instantaneous acceleration recorded at any GMV-D iteration, a_0 .

GMV-D requires that the system be initialized while the MARG is static (and in a location where the geomagnetic field is undistorted). Furthermore, it is established

that the orientation of the MARG body frame at startup will become the default inertial frame of reference (with respect to which the orientation of the MARG body frame will be characterized in all future iterations). According to that operational requirement, $A_{\rm INIT}$ should, indeed, be exclusively a reflection of the gravitational acceleration. But, expectedly, there will be some iterations in which the MARG will be in motion and, therefore, its accelerometer axes will report the superposition of gravity components and the corresponding "linear accelerations". It follows that, in iterations when the MARG is far from static, an accelerometer-based correction of the type contemplated in GMV-D should not be applied in full strength, and instead should be significantly restrained. This restraint on the accelerometer-based corrections is accomplished in GMV-D by having a single scalar parameter, $0 \le \alpha \le 1$, control the SLERP interpolation from the uncorrected $q_{\rm G}$ to the "fully corrected" $q_{\rm GA}$, yielding $q_{\rm SA}$, where accelerometer-based corrections which do not fulfill the necessary precondition (i.e., when $\alpha \approx 0$) will be essentially bypassed.

Accordingly, α must parametrize the level of (approximate) immobility of the MARG. In our work, we have used the Yost Labs 3-space USB MARG module, which internally computes a Confidence Factor, from 0 to 1, that can be read by issuing a command to the MARG and indicates "how much the sensor is being moved at the moment. This value will return 1 if the sensor is completely stationary and will return 0 if it is in motion. This command can also return values in between indicating how much motion the sensor is experiencing." [24]. Therefore, we compute α by reading this parameter and simply applying a linear function to precipitate the decrease of α when the MARG departs even slightly from immobility (and re-enforcing the lower bound of 0 and the upper bound of 1, in α). We have confirmed that, for other MARG modules that may not output such a Confidence Factor, one can be derived from the variance of the accelerometer axes and the gyroscope axes [14].

3.2 Original Magnetometer Correction Trustworthiness, µ

In the case of the two "vector observations" made on the geomagnetic field within the operating space of the MARG, the violation of the field uniformity assumption is not due to a sensor ambiguity. In this case the actual magnetic field is, actually, not uniform in some regions of space. A local distortion of the magnetic field may occur because of the presence of an object which produces an additional magnetic field of its own (e. g., permanent magnet). A local magnetic field distortion may even be due to a ferromagnetic object which simply provides a path of lower magnetic permeability to the lines of magnetic flux, causing them to experience detours. Whichever the cause, the magnetic vector in the neighborhood of these magnetic disruptors will likely be different in direction and/or magnitude from the geomagnetic field, which is uniform within the reduced operating volume that we would contemplate for a human-computer interaction application of the MARG module. Unfortunately, contemporary built environments (dwellings, offices, laboratories, etc.) are bound to be constituted in part by structural elements containing these magnetic disrupters. In addition, many types of contemporary furniture pieces (e.g., desks, filing cabinets, etc.) will also contain ferromagnetic components, such that distortions of the geomagnetic field in the operating space of the

MARG, and their associated negative impacts on orientation estimates, cannot be ruled out [15, 19, 20].

On the other hand, within the prospective use of the MARG for human-computer interaction, the assumption may be made that those magnetic disrupters will likely be at constant locations (or moving slowly) within the operating space of the MARG. Accordingly, we previously sought to consider the level of distortion of the geomagnetic field as a function of the spatial location of a point, or rather a small "voxel" (e.g., 2 x 2 x 2 cm.), being considered. This initially seemed an appealing approach when we were developing a system for orientation and position tracking of the MARG module, utilizing a 3-infared-camera system (OptiTrack V120 Trio) to read the real-time X, Y, Z position of an infrared reflective marker attached to the MARG module. Having available the X, Y, and Z position of the MARG every time its orientation was estimated allowed us to, under some circumstances, assign a µ value to the "current voxel" and store it in a 3-dimensional map of the μ values within the expected operating space of the MARG (meant to be attached to a glove worn by the computer user, for that previous application). For the sake of caution, the μ value of all the voxels would be initialized to a value of 0, so that the magnetic corrections would be "blocked" in regions of space for which the system did not yet have evidence of an acceptable magnetic trustworthiness (μ close to 1).

During each iteration, GMV-D would first determine if the value of α is above a minimum threshold (exclusively for this purpose), $\alpha > \alpha_{THR}$. Only if that is the case, such that the accelerometer-based correction, q_{GA} , can be considered to represent the true MARG orientation, the process of calculating a μ value for the current voxel could proceed. If the current value of α is found to be adequate, the accelerometer-corrected orientation, q_{GA} , can be used to map M_{INIT} to the current MARG body frame, yielding a computed magnetic vector $m(q_{GA})$, which should (ideally, in the case in which there is no magnetic distortion at the current location of the MARG), closely approximate the direction determined by the current readings of the 3 magnetometer axes, in vector m_0 .

In general, the cosine of the 3-dimensional angle between the directions of $m(q_{GA})$ and m_0 , that is, $\cos(\gamma)$, can be found computing their dot product. That cosine is already a parametrization of the direction disparity of the computed magnetic vector and the actual magnetometer readings, with values from -1 (totally opposite directions) to + 1 (exactly the same direction). Associating that directional disparity to the magnetic distortion in the current location of the MARG, a decrease of $\cos(\gamma)$ from + 1 towards -1 would indicate the presence of a proportionally significant magnetic distortion at the current location of the MARG. The corresponding value of $0 \le \mu \le 1$ is computed by first applying a linear function to $\cos(\gamma)$, in order to more severely penalize any decrease from the ideal value of + 1, and then overwriting any negative results with a value of 0. A more detailed explanation of this initial formulation of μ , with the involvement of the positional information provided by the 3-infrared-camera system, can be found in [18].

3.3 New, Self-contained Magnetometer Correction Trustworthiness, μ_K

While the conceptualization of the magnetic distortion level, and consequently, the μ value as a function of X, Y, Z location is appealing from the physical point of view and could lead to the development of "re-usable" μ maps in cases where the MARG

system is utilized repeatedly in the same room without frequent furniture re-assignments, it has a significant affordability drawback. MEMS MARG modules are particularly attractive in many circumstances due to their low cost (less than \$20 USD for each wired module, bought in large quantities). But the involvement of a calibrated multi-IR-camera setup immediately raises the prospective overall cost of a combined tracking system. In addition to its higher cost, a system that requires multiple cameras would increase the time and complexity of the corresponding setup process.

Therefore, we have tackled the challenge of defining a new, alternative magnetometer-correction trustworthiness parameter, which we have designated as μ_K , that does not require any type of information from devices that are external to the MARG module under consideration. That is, we have developed a "self-contained" implementation of GMV-D where the new μ_K is used.

The goal in the development of μ_K and its use in GMV-D is to detect when the MARG has entered an area with significant distortion of the geomagnetic field, prior to the computation of the final orientation estimate of MARG orientation, q_{OUT} , for the current iteration. Accordingly, we will consider the human-computer interaction context in which the MARG is being used and leverage the (relatively) low range of speeds in the hand movements of a human computer user, so that we can adopt (tentatively, and just for the purpose of μ_K computation) the q_{OUT} estimation resulting from the *previous* iteration, which we will designate $q_{OUTprev}$, as a useful approximation to the MARG orientation in the current iteration.

Under this assumption, we will "map back" the magnetic vector sensed in this iteration, \mathbf{m}_0 , to the inertial reference frame, resulting in the vector \mathbf{m}_{0i} :

$$\mathbf{m}_{0i} = \mathbf{q}_{OUTprev} \otimes \mathbf{m}_{0} \otimes \mathbf{q}_{OUTprev}^{*} \tag{13}$$

This is necessary, so that the currently detected magnetic field *referenced to the inertial frame* can be properly compared against the initial (undistorted) magnetic vector recorded at startup, $M_{\rm INIT}$, which is also referenced to the inertial frame. Once both magnetic vector directions are referenced to the same (inertial) frame we develop two intermediate parameters, $\mu_{\rm KA}$ and $\mu_{\rm KM}$, which quantify the discrepancies in terms of angles and magnitudes between $M_{\rm INIT}$ and $m_{\rm oi}$, respectively.

The angular discrepancy is first assessed as the angle λ between the vectors through their inner product:

$$\lambda = \cos^{-1} \left[\frac{\boldsymbol{M}_{INITit} \cdot \boldsymbol{m}_{0i}}{||\boldsymbol{M}_{INIT}|| ||\boldsymbol{m}_{0i}||} \right]$$
 (14)

Based on λ , we have formulated μ_{KA} to drop faster as the angle departs its ideal value of 0 (which would indicate no angular discrepancy, likely due to the absence of magnetic distortion). This is implemented through this linear equation:

$$\mu_{KA} = 1 - 1.5\lambda \tag{15}$$

In order to formulate μ_{KM} as a more specific quantification of the magnitude discrepancies between M_{INIT} and m_{oi} , we defined a "penalty" parameter that grows from 0 only when it takes place simultaneously with considerable misalignment between M_{INIT} and

 m_{oi} , which is more likely attributable to actual magnetic distortion in the magnetic field currently sensed by the MARG:

$$penalty = \left\lceil \frac{||\boldsymbol{m}_{0i}||}{||\boldsymbol{M}_{init}||} \right\rceil (\lambda) \tag{16}$$

and

$$\mu_{KM} = 1 - penalty \tag{17}$$

where any negative results for μ_{KM} will be overwritten with a value of 0.

The fusion of μ_{KA} and μ_{KM} takes place in a few steps, starting with the average of, μ_{KA} and μ_{KM} to define an intermediate result μ_1 :

$$\mu_1 = [\mu_{KA} + \mu_{KM}]/2 \tag{18}$$

This intermediate parameter μ_1 is channeled through a First-In-First-Out (FIFO) structure, so that the current and immediately previous 5 values are available in any iteration. From these group of μ_1 values the minimum is extracted as μ_2 . This is done so that spurious transient increases in the instantaneous value of μ_1 will still not be allowed to apply a strong magnetic correction, reserving that possibility for instances when μ_1 has been consistently high.

Finally, μ_K is obtained using μ_2 as a factor, where the other factor is α . This serves as a blocking mechanism that will "disable" large values of μ_2 computed during rapid movements which would be in violation of the initial assumption of slow or moderate motion (I.e., when α is not close to 0, we can better justify the use of $q_{OUTprev}$ as a valid approximation of the current MARG orientation).

$$\mu_K = (\mu_2)(\alpha) \tag{19}$$

4 Evaluation Protocol

4.1 Setup

We sought to assess the level of resilience that the GMV-D, with the newly formulated μ_K , would exhibit in estimating MARG orientation even in regions of space with known significant magnetic distortion. To that end, we designed a sequence of translations and rotations of the MARG that includes manipulations in both a magnetically undistorted area (A) and a magnetically distorted area (B), with the sequence starting and ending at a third position (also undistorted) that acted as "home location" (H). The Yost 3-Space Mini Wireless MARG module we used follows the "left-hand coordinate" convention, by default, and recorded data at sampling intervals of 70 ms. The 3 locations were arranged as a (horizontally) mirrored "L", with location (A) at the intersection of the 2 strokes of the L. The H-to-A stroke was approximately 30 cm. in length and ran North-to-South. The A-to-B stroke was approximately 40 cm. in length and ran East-to-West. The setup was placed away from iron furniture and all the necessary supports were made of wood. To create the magnetic distortion at B, a 0.5 x 3.8 x 37.5 cm steel bar was placed at B, right under a horizontal cardboard that served as a horizontal plane reference where H, A and B were located.

4.2 Manipulation Sequence and Poses

In each testing run, the MARG would be initialized (startup) at H, under magnetically undistorted and static conditions, as required by the algorithm. The module case laid flat with its "thickness" (its -Y axis) parallel to the plumb line ("POSE_1"). Then the following actions would be taken in the first half of the test run (not magnetically distorted):

```
Translation without rotation, H to A, keeping POSE_1 orientation throughout + 90° rotation about the Z body axis, defining POSE_2, and return to POSE_1 + 90° rotation about the X body axis, defining POSE_3, and return to POSE_1 + 90° rotation about the Y body axis, defining POSE_4, and return to POSE_1 Combined + 90° in X and - 45° in Y, defining POSE_5, and return to POSE_1
```

Then the MARG would be translated, without rotation, from A to B (landing in POSE_6, which is the same orientation as POSE_1) and the sequence described above would be replicated exactly, but now in B, i.e., within the magnetically distorted region:

- + 90° rotation about the Z body axis, defining POSE_7, and return to POSE_6
- + 90° rotation about the X body axis, defining POSE_8, and return to POSE_6
- + 90° rotation about the Y body axis, defining POSE_9, and return to POSE_6
- Combined + 90° in X and 45° in Y, defining POSE_10, and return to POSE_6

Finally, the MARG would be translated, without rotation, from B to H.

The resilience of a given orientation estimation algorithm can then be assessed by the similarity of the results obtained for poses 1-trough-5, in the magnetically undistorted region (A), in which most algorithms will provide satisfactory orientation estimates, and the results obtained for poses 6-through-10, in the magnetically distorted environment (B).

In the next section we display the time evolution of the orientation estimation quaternion components obtained from GMV-D, with μ_K , as well as those from benchmark orientation estimations: Kalman Filter [22] (computed within the YOST 3-Space MARG), and the Madgwick [5] and Mahony [6] algorithms, implemented in Matlab, as made available by Sebastian Madgwick at: at https://x-io.co.uk/open-source-imu-

and-ahrs-algorithms/. (Since the Matlab implementations posted by Madgwick are for a sensor that follows the "right-handed" coordinate convention, the sensor data directions needed to be reassigned and "re-sampling" had to be performed to obtain data sequences at an equivalent sampling rate of 256 Hz, which is the condition expected by the implementations provided in the website. Similarly, the output quaternion components needed to be re-organized.)

5 Results and Discussion

This section presents the results obtained from the GMV-D algorithm, using the newly proposed μ_K parameter for two representative sequences of manipulations which followed the schedule described in Subsect. 4.2. For each one of the sequences, we first present the evolution of the novel parameter μ_K and its μ_{KA} and μ_{KM} components, accompanying the evolution of quaternion components from GMV-D and from the on-chip implementation of a Kalman Filter (KF). Then we compare the quaternion evolution from GMV-D with the corresponding results from two other contemporary methods.

5.1 Results from Two Experimental Sequences

Figure 2 displays on its top panel the evolution of the values of the components μ_{KA} and μ_{KM} , the overall novel parameter μ_{K} and the evolution of the 4 components of the orientation quaternion computed by GMV-D, where the timing of the poses held in the magnetically undistorted region (A) is indicated by blue underlined numbers (1, 2, 3, 4, 5), and the timing of the poses held in the magnetically distorted region (B) is indicated by red underlined numbers (6, 7, 8, 9, 10). For comparison, the evolution of the quaternion components calculated by the on-chip Kalman Filter are also shown. It should be noted, in this top panel, that both GMV-D and KF report essentially the same quaternions for the first part of the record (poses 1, 2, 3, 4, 5), which were held in the magnetically undistorted area. However, for the poses held in the magnetically distorted area (poses 6, 7, 8, 9, 10), the results from GMV-D and KF differ considerably. Since the sequence of orientations is the same as for the first part of the record, the GMV-D output seems correct as it closely resembles the patterns generated for the first half. In contrast, the KF output for the second half is markedly different from its output for the first half, indicating that the KF orientation estimator has succumbed to the presence of the magnetic distortion in B. It is also interesting to note that GMV-D is disregarding the prospective magnetometer-based corrections during poses 6, 7, 8, 9, 10, as evidenced by the zero value acquired by μ_K during that interval.

The bottom panel of Fig. 2 serves the purpose of comparing the evolution of components from the GMV-D quaternion (showed, again, with the timing of the poses indicated by underlined numbers), to the evolutions of quaternions generated from the same accelerometer, gyroscope and magnetometer data by the Madgwick and Mahony algorithms. The same comments made above for the output of the Kalman Filter apply to the outputs of these two other algorithms. All in all, these figures confirm that GMV-D has displayed a much higher level of resilience to the distortion of the magnetic field, by appropriately suppressing (μ_K close to 0) the involvement of the magnetometer signals in the correction of the initial orientation derived by integration of the gyroscope signals.

The two panels in Fig. 3 are organized in the same way as for Fig. 2 and simply present the results from a different experimental run, where the timing of the rotations in the same sequence is slightly different. The same general behavior and conclusions derived from Fig. 2 apply to Fig. 3 as well.

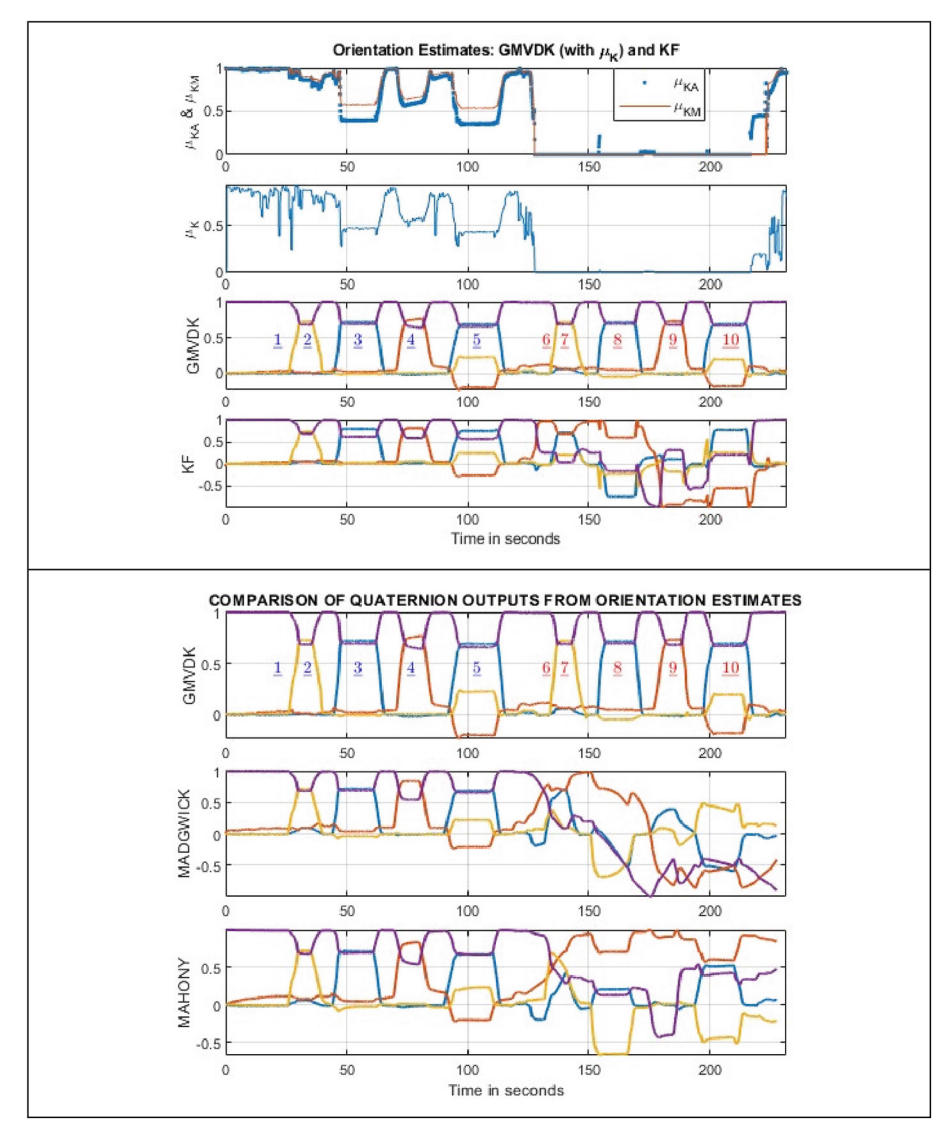


Fig. 2. – Record 1 [TOP] Time evolution of the μ_K magnetometer trustworthiness parameter and its components μ_{KA} and μ_{KM} , along with the 4 components of the resulting orientation quaternion produced by GMV-D. The blue underlined numbers indicate the timing of the poses held in the magnetically undistorted location. The red underlined numbers indicate the timing of the poses held in the magnetically distorted location. The 4 quaternion components generated by a Kalman Filter are shown for comparison. [BOTTOM] Components of the GMV-D quaternion are compared with those generated by the Madgwick and Mahony algorithms.

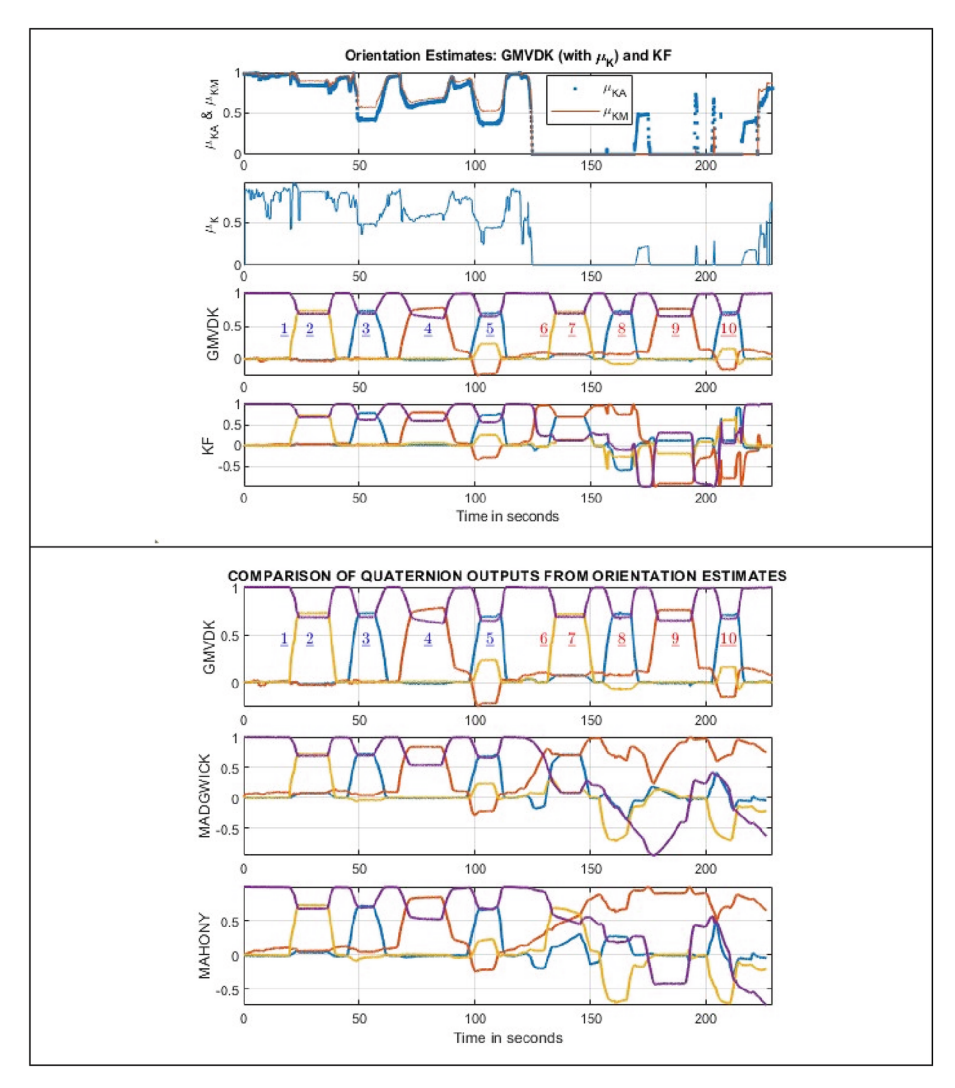


Fig. 3. – **Record 2** [TOP] Time evolution of the μ_K magnetometer trustworthiness parameter and its components μ_{KA} and μ_{KM} , along with the 4 components of the resulting orientation quaternion produced by GMV-D. The blue underlined numbers indicate the timing of the poses held in the magnetically undistorted location. The red underlined numbers indicate the timing of the poses held in the magnetically distorted location. The 4 quaternion components generated by a Kalman Filter are shown for comparison. [BOTTOM] Components of the GMV-D quaternion are compared with those generated by the Madgwick and Mahony algorithms.

5.2 Discussion

The top panel of Figs. 2 and 3 confirm that the newly proposed μ_K parameter effectively drops to 0 during the portion of the recordings in which the MARG was in the neighborhood of the magnetically distorted location, B. Both the μ_{KA} and μ_{KM} components

display a sharp decrease and the resulting μ_K is effectively cancelled during that interval. The evolution of the quaternion components from GMV-D and from KF show that both algorithms yield very similar results during the first half of the record (while the MARG was in a magnetically undistorted area) but display very different results for the second half of the record. It can be observed that the GMV-D results closely resemble the results it generated during the first half, even when the MARG was now located in the magnetically distorted area. This is reasonable, since the sequence of rotations performed in B was the same as the sequence of rotations performed in A. Therefore, it is the KF method which is yielding erroneous results during the second part of the recording, while the MARG was in the magnetically distorted location (B).

The bottom panels of Figs. 2 and 3 provide further confirmation of the resilience of GMV-D to magnetic distortions, by comparing the evolution of the orientation quaternion components from GMV-D to those that were obtained from the Madgwick and Mahony methods for the same MARG data. Here, again, all three methods yield similar orientation estimates while the MARG operated in location A (magnetically undistorted) but generated very different orientation estimates for location B (magnetically distorted region). Since the sequence of rotations was the same in B as it was in A, the unfamiliar quaternion components produced by Madgwick and Mahoney indicate that these methods had limited robustness to the presence of magnetic distortions.

6 Concluding Remarks

The results from two prototypical test runs shown and discussed in the previous sections seem to confirm that the new "self-contained" version of GMV-D is more resilient to the existence of magnetically distorted regions in the operating space for the MARG than some classical (KF) and contemporary (Madgwick, Mahony) orientation estimation algorithms.

The autonomy gained by GMV-D through the new formulation of μ_K is important at the conceptual and practical levels. Conceptually, it has presented a plausible mechanism to identify the suspected occurrence of local magnetic distortion from the sensors contained in the MARG alone, leveraging the appropriateness of one modality (i.e., iterations with large-enough α), when available, to evaluate the appropriateness of a different modality (i.e., to compute μ_K as a trustworthiness parameter for the magnetometer information). Practically, the "self-contained" character of the new version of GMV-D relieves potential users of this approach pursuing only the determination of orientation from having to include in the setup a typically much more expensive position tracking device. Furthermore, the new GMV-D might be suitable for pairing with a lower-resolution position tracking system when seeking the combined determination of position and orientation. In that respect, the new version of GMV-D may finally allow the utilization of MARG sensors for human-computer applications such as hand-tracking without a strong dependency on particularly expensive high-end vision tracking components.

Acknowledgments. This work was supported by the US National Science Foundation grants CNS-1532061 and CNS-1920182.

References

- Abyarjoo, F., Barreto, A., Abyarjoo, S., Ortega, F.R., Cofino, J.: Monitoring human wrist rotation in three degrees of freedom. In: 2013 Proceedings of IEEE Southeastcon, pp. 1–5 (2013)
- Hanson, A.: Visualizing Quaternions. Morgan Kaufmann Series in Interactive 3D Technology.: Morgan Kaufmann. Elsevier Science distributor, Boston, p. 498 (2006)
- 3. Johnson, R.C.: 3-Axis MEMs gyro chip debuts. EE Times (2009). https://www.eetimes.com/ 3-axis-mems-gyro-chip-debuts/
- 4. Kuipers, J.B.: Quaternions and rotation sequences: a primer with applications to orbits, aerospace, and virtual reality, p. 371. Princeton University Press, Princeton, N.J, xxii (1999)
- Madgwick, S.: An efficient orientation filter for inertial and inertial/magnetic sensor arrays.
 Report x-io and University of Bristol (UK) 25, pp. 113-118 (2010)
- 6. Mahony, R., Hamel, T., Pflimlin, J.-M.: Nonlinear complementary filters on the special orthogonal group. IEEE Trans. Autom. Control **53**(5), 1203–1218 (2008)
- Markley, F.L., Mortari, D.: Quaternion Attitude Estimation Using Vector Observations. J. Astronaut. Sci. 48(2–3), 359–380 (2000). https://doi.org/10.1007/BF03546284
- 8. O-larnnithipong, N.: Hand motion tracking system using inertial measurement units and infrared cameras. In: Electrical and Computer Engineering Department. Florida International University, Miami, Florida, USA (2018)
- O-larnnithipong, N., Barreto, A.: Gyroscope drift correction algorithm for inertial measurement unit used in hand motion tracking. IEEE SENSORS. 2016, 1–3 (2016)
- O-larnnithipong, N., Barreto, A., Tangnimitchok, S., Ratchatanantakit, N.: Orientation correction for a 3D hand motion tracking interface using inertial measurement units. In: Kurosu, M. (ed.) HCI 2018. LNCS, vol. 10903, pp. 321–333. Springer, Cham (2018). https://doi.org/10.1007/978-3-319-91250-9_25
- O-larnnithipong, N., Barreto, A., Ratchatanantakit, N., Tangnimitchok, S., Ortega, F.R.: Real-time implementation of orientation correction algorithm for 3D hand motion tracking interface. In: Antona, M., Stephanidis, C. (eds.) UAHCI 2018. LNCS, vol. 10907, pp. 228–242. Springer, Cham (2018). https://doi.org/10.1007/978-3-319-92049-8_17
- 12. Nonnarit, O., Ratchatanantakit, N., Tangnimitchok, S., Ortega, F., Barreto, A.: Hand tracking interface for virtual reality interaction based on MARG sensors. In: 2019 IEEE Conference on Virtual Reality and 3D User Interfaces (VR), pp. 1717–1722 (2019)
- O-larnnithipong, N., Ratchatanantakit, N., Tangnimitchok, S., Ortega, F.R., Barreto, A., Adjouadi, M.: Statistical analysis of novel and traditional orientation estimates from an IMU-instrumented glove. In: Antona, M., Stephanidis, C. (eds.) Universal Access in Human-Computer Interaction. Multimodality and Assistive Environments. HCII 2019. Lecture Notes in Computer Science(), vol. 11573, pp. 282–299. Springer, Cham (2019). https://doi.org/10. 1007/978-3-030-23563-5_23
- Ratchatanantakit, N.: Digital processing of magnetic, angular-rate, and gravity signals for human-computer interaction. In: Electrical and Computer Engineering Department, Florida International University, Miami, Florida, USA (2021)
- Ratchatanantakit, N., O-larnnithipong, N., Barreto, A., Tangnimitchok, S.: Consistency study of 3D magnetic vectors in an office environment for IMU-based hand tracking input development. In: Kurosu, M. (ed.) HCII 2019. LNCS, vol. 11567, pp. 377–387. Springer, Cham (2019). https://doi.org/10.1007/978-3-030-22643-5_29
- Ratchatanantakit, N., Nonnarit, O., Sonchan, P., Adjouadi, M., Barreto, A.: Live demonstration: double SLERP gravity-magnetic vector (GMV-D) orientation correction in a MARG sensor. In; 2021 IEEE Sensors, p. 1 (2021)

- Ratchatanantakit, N., O-larnnithipong, N., Sonchan, P., Adjouadi, M., Barreto, A.: Statistical evaluation of orientation correction algorithms in a real-time hand tracking application for computer interaction. In: Kurosu, M. (eds.) Human-Computer Interaction. Technological Innovation. HCII 2022. Lecture Notes in Computer Science, vol. 13303, pp. 92–108. Springer, Cham (2022).https://doi.org/10.1007/978-3-031-05409-9_8
- 18. Ratchatanantakit, N., O-larnnithipong, N., Sonchan, P., Adjouadi, M., Barreto, A.: A sensor fusion approach to MARG module orientation estimation for a real-time hand tracking application. Inf. Fusion **90**, 298–315 (2023)
- 19. Roetenberg, D., Luinge, H., Veltink, P.: Inertial and magnetic sensing of human movement near ferromagnetic materials. In: Second IEEE and ACM International Symposium on Mixed and Augmented Reality 2003, pp. 268-269. IEEE (2003)
- Roetenberg, D., Luinge, H.J., Baten, C.T.M., Veltink, P.H.: Compensation of magnetic disturbances improves inertial and magnetic sensing of human body segment orientation. IEEE Trans. Neural Syst. Rehabil. Eng. 13(3), 395–405 (2005)
- 21. Shoemake, K.: Animating rotation with quaternion curves. SIGGRAPH Comput. Graph. **19**(3), 245–254 (1985)
- 22. Simon, D.: Kalman filtering. Embedded systems programming, vol. 14, no.6, pp. 72–79 (2001)
- 23. Vince, J.: Quaternions for Computer Graphics. Springer, New York, p. xiv, p. 140 (2011)
- 24. YostLabs 3-Space Sensor Miniature Attitude & Heading Reference System with Pedestrian Tracking User's Manual (2017)